Thermal Science and Engineering Progress 39 (2023) 101693

Contents lists available at ScienceDirect

Thermal Science and Engineering Progress

journal homepage: www.sciencedirect.com/journal/thermal-science-and-engineering-progress

Experimental and computational analysis of thermoelectric modules based on melt-mixed polypropylene composites

Qusay Doraghi [a], Alina Żabnieńska-Góra [a,b], Les Norman [a], Beate Krause [c], Petra Pötschke [c], Hussam Jouhara [a,d,*]

[a] Heat Pipe and Thermal Management Research Group, College of Engineering, Design and Physical Sciences, Brunel University London UB8 3PH, UK
[b] Wroclaw University of Science and Technology, Faculty of Environmental Engineering, Wybrzeze Wyspianskiego 27, 50-370 Wroclaw, Poland
[c] Department of Functional Nanocomposites and Blends, Leibniz-Institut für Polymerforschung Dresden e.V. (IPF), Hohe Str. 6, 01069 Dresden, Germany
[d] Vytautas Magnus University, Studentu Str. 11, LT-53362, Akademija, Kaunas Distr., Lithuania

ARTICLE INFO

Keywords:
Thermoelectric generators
New TEG leg geometries
Melt-mixed polypropylene composites
COMSOL simulation
Validation of TEG model

ABSTRACT

Researchers are constantly looking for new materials that exploit the Seebeck phenomenon to convert heat into electrical energy using thermoelectric generators (TEGs). New lead-free thermoelectric materials are being investigated as part of the EU project InComEss, with one of the anticipated uses being converting wasted heat into electric energy. Such research aims to reduce the production costs as well as the environmental impact of current TEG modules which mostly employ bismuth for their construction. The use of polymers that, despite lower efficiency, achieve increasingly higher values of electrical conductivity and Seebeck coefficients at a low heat transfer coefficient is increasingly discussed in the literature. This article presents two thermoelectric generator (TEG) models based on data previously described in the literature. Two types of designs are presented: consisting of 4- and 49-leg pairs of p- and *n*-type composites based on polypropylene melt-mixed with single-walled carbon nanotubes. The models being developed using COMSOL Multiphysics software and validated based on measurements carried out in the laboratory. Based on the results of the analysis, conductive polymer composites employing insulating matrices can be considered as a promising material of the future for TEG modules.

Introduction

Energy efficiency is one of the key factors for a sustainable energy policy and there are many approaches to improving the energy efficiency of equipment or systems – one of these being waste heat recovery. Waste heat is generated as a by-product of many production processes, and when not re-used, it dissipates this heat into the atmosphere or into water. Appropriately, waste energy management is a far-reaching current issue, and heat recovery is used both in industrial production plants for such as aluminium, ceramics or steel [1,2]; the cement industry [3]; for mechanical ventilation systems in residential buildings [4], as well as in individual appliances such as rotary kiln shell [5]; proton exchange membrane fuel cells [6], or PVT collectors [7,8]. This waste energy is not only neutral in terms of carbon dioxide emissions and pollutants discharged into the environment, but also saves primary fuel. There are a number of technologies for utilising waste heat or that are part of a thermal management system, for example: the Organic Rankine Cycle (ORC) [9,10], heat pipes [11–14], heat pumps, as well as thermoelectric generators (TEGs) [15–17]. TEG technology is currently-one of the most interesting proposals, because, using this, it is possible to convert waste heat directly into electrical energy via a thermoelectric phenomena.

InComEss aims to produce efficient smart materials with energy harvesting and storage capabilities by merging innovative polymer-based composite materials into a revolutionary single/multisource approach to collect electrical energy from mechanical energy and/or waste heat environmental sources [18].

In the past, thermoelectric (TE) devices were mainly based on the Peltier phenomenon and were used in refrigeration applications, but currently TE generator (TEG) modules are increasingly exploiting the Seebeck phenomenon which enables waste heat to be converted into electricity. The Seebeck effect occurs when there is a temperature difference between the two sides of the generator (cold and hot sides)

* Corresponding author at: Heat Pipe and Thermal Management Research Group, College of Engineering, Design and Physical Sciences, Brunel University London UB8 3PH, UK.
E-mail address: hussam.jouhara@brunel.ac.uk (H. Jouhara).

https://doi.org/10.1016/j.tsep.2023.101693
Received 9 November 2022; Received in revised form 31 January 2023; Accepted 31 January 2023
Available online 2 February 2023

which causes the diffusion of charge carriers (electrons or holes) along the material. The maximum efficiency (η_{max}) depends on both the Carnot efficiency and a dimensionless thermoelectric *Figure of merit* (zT) as shown in Eq. (1). where T_h, T_c are temperatures of hot-end, cold-end respectively.

$$\eta_{max} = \frac{T_h - T_c}{T_h} \cdot \frac{\left(\sqrt{1+zT}\right) - 1}{\left(\sqrt{1+zT}\right) + \frac{T_c}{T_h}} \quad (1)$$

The Figure of merit combines the three most important parameters that characterise thermoelectric materials – the Seebeck coefficient S, electrical conductivity σ and the thermal conductivity κ – all combined with the T absolute temperature according to the following formula:

$$zT = \frac{S^2 \sigma T}{k} \quad (2)$$

where $S^2\sigma$ is defined as the Power Factor PF [19].

According to equation (2), suitable materials used for the construction of the TEG are be characterised by high electrical conductivity, a high absolute value of the Seebeck coefficient (for maximum conversion of heat to electrical power – which can be *n*-type (negative – electrons) or p-type (positive - holes) as a function of the dominant type of charge carrier), and low thermal conductivity [16]. In addition, the main thermoelectric materials properties of electrical conductivity and Seebeck coefficient are temperature dependent, and they usually present the highest zT within a specified temperature range. Furthermore S, σ and κ are all interdependent as a function of material band structure, microstructure or carrier concentration (Fig. 1) [20]. Improving zT is still therefore a challenge.

Strategies for increasing the Seebeck coefficient and electrical conductivity are widely discussed in the literature [21–23]. Mao et al. [24] for example, focused on discussing strategies for enhancing thermoelectric performance considering among others: carrier concentration optimization, suppression of the bipolar conduction, phonon engineering, carrier mobility and Seebeck coefficient enhancement.

In order to increase the widespread use of thermoelectric materials for various applications, researchers are looking for thermoelectric materials with the highest possible zT values but that are also environmentally safe and cost-effective to produce.

where $S^2\sigma$ is defined as the Power Factor PF [19].

za [20]. Improving zT is still therefore a challenge.

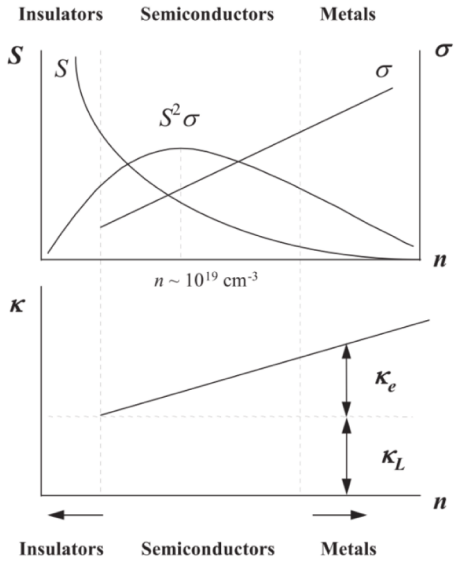

Fig. 1. Dependence of the main material properties (S, σ and κ_L (lattice thermal conductivity), κ_e (electrical thermal conductivity)) on carrier concentration. Reproduction with permission from Qiu et al. [20].

According to report [25], the thermoelectric generator market is segmented, on the basis of materials, into bismuth telluride, lead telluride and others, with bismuth telluride being the most widely used material – its share being projected to increase by a further 12 % in 2030 compared to 2020. For Bi_2Te_3 alloys (depending on the temperature range) the zT is limited to the range 0.7–1.4 because it is difficult to reduce the high thermal conductivity of these materials [26]. In addition, despite the widespread use of Bismuth telluride and lead telluride there are doubts regarding the toxicity and the availability of individual elements. Furthermore, their rigidity and high production cost limit the possible applications. Another group of compounds that could be used for TEG applications are Cu-based thermoelectric materials and currently, the zT of Cu-based TE materials have exceeded 2.0 [20]; however, they are typically used at high temperatures of approx. 1000 °C which limits their application.

So overall, polymer based materials, despite having currently only a very low share [19], are perhaps a better alternative to the previously mentioned materials [26]. They are widely available, can be easily processed into different shapes even at large scale, have a much lower production and processing costs and, most importantly, have intrinsically low thermal conductivity – one of the desired TE parameters. This article therefore discusses the use of thermoplastic polymer composites for TE application and presents a TEG model (built using the COMSOL Multiphysics Software) for previously published examples consisting of polypropylene-based melt mixed composites with single-walled carbon nanotubes. The model is then validated by comparison with measured data for these TEG modules [27].

Thermoelectric materials based on thermoplastic polymer composites

In the context of increasing demand for environmentally friendly, lightweight and easy-to-process TE materials, polymer-based materials are also showing promise [28–32]. They also have the advantages of being cheap, with no geopolitical supply risks and an inherently low thermal conductivity. In addition to intrinsically conductive polymers [30] (which have to be doped and are not always easy to process), conductive polymer composites (CPCs) have been increasingly investigated in recent years for their thermoelectric properties [29]. For industrial applications, thermoplastic polymers are particularly interesting because they can be processed in the melt and can then easily moulded into various structures and shapes – such as films, blocks, and textiles – and are easily scalable. In addition, compared to the traditional structures using metal oxide blocks, the pliant nature of such mechanically flexible materials means that yet more new designs can be realised [33,34].

To be used as a TE material, the polymers must be electrically conductive. So, in CPCs, conductive fillers such as carbon fibres, carbon black, graphite and graphene structures or carbon nanotubes (CNTs) are added in such quantities that they form an electrically conductive network within the matrix. Fortunately, such networks can be formed using relatively small amounts of filler [35] so that the thermal conductivity is not significantly increased. The amount required to reach the electrical percolation threshold (beyond which conductivity strongly increases for even a small increment in filler loading) depends very much on the filler aspect ratio and is lower the higher the filler ratio. In this context, CNTs with aspect ratios up to 1000 and above are very favourable and require contents in the range of less than 1 wt% for percolation and in the range of 2–5 wt% for suitable electrical conductivities [35]. Such low levels also have no significant effect on mechanical flexibility or other properties. However, a major disadvantage of CPCs with CNTs is that their electrical conductivity is significantly lower than other typically used TE materials, such as Bi_2Te_3, although the Seebeck coefficients of melt-mixed composites can be in the range of

up to 66 μV/K (e.g. for polybutylene terephthalate (PBT) with 7 wt% SWCNT) or −57 μV/K (for acrylonitrile butadiene styrene (ABS) with 0.5 wt% SWCNT) [36].

The research on melt-mixed thermoplastic CPCs for TE application began around 2010 and the first reports by Antar et al. [37] discussed p-type poly(lactid acid) (PLA) based composites with multiwalled CNTs (MWCNTs) and expanded graphite (eGr) with Seebeck coefficients of around 18 μV/K at eGr fillings of 10–30 vol%. Melt mixed polycarbonate (PC)-based composites were presented by Liebscher et al. [37,38] with S values of about 14 μV/K. Poly (vinylidene fluoride) (PVDF) composites with 8 wt% MWCNTs were shown by Sun et al. [39] to have S values of 10 μV/K, and after foaming, a slight reduction was found. For those with 5–15 vol% graphene nanoplatelets (GNPs) values of about 28 μV/K were measured which after foaming improved significantly up to 58 μV/K. First reports on using single-walled CNTs (SWCNTs) in melt-mixed polypropylene (PP) based composites were reported by Luo et al. At the very low loading of 0.8 wt% SWCNTs and the addition of 5 wt% of copper oxide (CuO, a material with a high S value), Seebeck coefficients up to 45 μV/K were reached [40].

Studies on the use of boron-doped SWCNTs showed that the TE properties of prepared PP based composites can be enhanced [41] and S-values of 59.7 μV/K were obtained for PP with 0.5 wt% B-SWCNT compared to 47.9 μV/K for SWCNTs at the same filling level. Furthermore, it was shown that with PP based composites the Seebeck values are not only dependent on the SWCNT content [40] and modifications [27] but also melt mixing conditions [27] and such derived differences in SWCNT dispersion and distribution and on the addition of solid [40] or liquid [27,42,43] additives. Other polymer matrices studied using melt-mixing with CNTs are polyamide 66 (PA66), polyamide 6 (PA6) and partially aromatic polyamide (PARA) [36].

To get *n*-type melt-mixed composites (as needed in effective TEG systems) different approaches were noted in published literature. In one method, nitrogen doped (*N*-doped) MWCNTs with negative S values were synthesized and incorporated in PP also resulting in the composites with negative S values [44]. The S values achieved were between −4.7 μV/K and −22.8 μV/K for composites with 1.5 wt% to 7.5 wt% *N*-MWCNT. Also, carbon nanofibers having negative S-values resulted in negative values of composites based on PP [45,46]. In addition, Luo et al. reported that the use of polyethylene glycol (PEG) as a low molecular additive directly in the melt-mixing process can lead to a switching of the sign of the S value [27] and resulted in S values of −56 μV/K for a composite of PP with 2 wt% SWCNT, 5 wt% CuO and 10 wt% PEG. Such switching agents could also be ionic liquids (as reported by Voigt et al.) who found a S value of −27.6_μV/K for PP/2 wt% SWCNT/4 wt% IL type 1-allyl-3-methyl-imidazolium chloride [47]. In addition, it was found that also certain polymer matrices can induce negative Seebeck values in composites containing p-type carbon nanofillers. This was found for solution mixing by Piao et al. [48] and for melt-mixing by Krause et al. [36]. The polymer matrices which can dope the SWCNTs (such as PA6, PA66, PARA and ABS), typically have nitrogen groups or amide structures.

Based on the developments with composites of PP with SWCNTs of the type Tuball (OCSiAl company), Luo et al. in 2017 presented a proof-of-concept demonstrator for two TE modules which are based on electrically conductive strips of melt-mixed and compression moulded composites [27]. The results showed that such polymer materials are, in principal, suitable for TE applications. Two simple designs were selected, the first using 4 pairs of p- and *n*-type strips mounted on two cooper blocks, leading to a thermovoltage of 21 mV for a 70 K temperature difference. In addition, based on the principle shown by Hewitt et al. [34], for the second, an accordion like structure based on 49p- and *n*-type pairs was constructed and tested which results in an output voltage of 110 mV. The p-type composite used in the modules consists of PP with 2 wt% SWCNTs and 5 wt% copper oxide – a composition which was shown from the result of a previous study to result in maximum of the power factor [40]. For *n*-type composites the same base material was used but for this 10 wt% PEG was added directly during the melt-mixing to achieve the *n*-type character; the amount being based on the research that a PEG:CNT ratio of 5:1 was shown to result in the highest value of PF [27]. These were the two proof-of-concept modules that are used (in this paper) to test the applicability of a simulation software concerning their TE behaviour.

Thermoelectric modelling and simulation

Model

Computer simulations have become an indispensable tool not only for designing and optimising technological processes but also for conducting scientific research. One such software is COMSOL Multiphysics – this software enabling the user to create models by: defining parameters, building geometry, applying physics, composing the mesh, solving the model and then visualising and postprocessing the results. It offers fully coupled multiphysics and single-physics modelling capabilities [49] and therefore allows the analysis of all occurring processes in the TEG and, at the same time, investigating the influence of the main parameters on electrical potential differences.

Numerous examples of TEG application have been published. For example: Satish and Nedumaran [50] simulated a small TEG for a handheld electric gadgets and in their research, COMSOL Multiphysics 4.2 was employed to achieve the best possible design parameters for manufacturing. Zeyu et al. [51] used COMSOL to generate a three-dimensional transient thermal-electric numerical model to precisely forecast the performance of a solar thermoelectric generator. Ding et al. [52] used COMSOL Multiphysics 5.4 to couple together available Fluid, Thermal and Electric multiphysics modules to establish a transient numerical modeling for a TEG system used for automotive exhaust waste heat recovery. Charilaou et al. [53] used COMSOL Multiphysics to model an air-cooled TEG system for use in cement industries. The authors analysed a three-dimensional model to identify the key parameters impacting the temperature difference along the side surface of the TEG modules. Ting et al. [54] used COMSOL Multiphysics 4.4 to generate a numerical investigation on 'thermoelectric-hydraulic performance of a thermoelectric power generator' to predict and evaluate a gas-to-liquid TEG model by arranging the laminar flow, heat transfer and electric current modules. Xuejian et al. [55] introduced 'an optimized design approach concerning thermoelectric generators with frustum-shaped legs based on three-dimensional multiphysics model'. Moreover, the software was previously used by our group (the Heat Pipe and Thermal Management Research Group,) to model and computationally investigate variable TEG leg geometry [56]. The analysis was conducted under steady-state conditions, with a multiphysics node added to the software which included Thermoelectric Effect and Electromagnetic Heating Multiphysics coupling features. Several different types of variable thermoelectric legs (i.e., Cone-leg and Diamond-leg) were computationally modelled, and their performance evaluated under steady-state conditions by two stages of investigation. At stage one, a TEG models made from two p- and *n*-type pairs was analysed and the impact of the new geometry on the thermal conductivity, electrical resistivity and the overall stress assessed. At the second research stage, using the COMSOL Multiphysics coupling features, the whole TEG module consisting of 128p- and *n*-pairs was modelled and the performance investigated.

Overall, the building of a TEG model and its validation is a very important step in analysing the generator performance. Its use significantly speeds up analysis of the electric potential differences for different thermoelectric material properties that use the same geometry. Validation consists in comparing the results of numerical simulations with experimental results. The purpose of this process is to quantify errors resulting from assumptions made in a model that has been solved numerically.

For the two proof-of-concept example TEG modules (described above), the modeling was performed using COMSOL Multiphysics 5.6

software and Fig. 2 demonstrates the steps taken when generating the modules. It should be noted that material data were taken from [27] or additionally obtained by the authors. The properties of the polymer composites used in further analyses are shown in the Table 1. Additionally, the measurement error for the Seebeck coefficient, electrical and thermal conductivity is provided.

Boundary conditions

Based on the information available within the literature [27] on laboratory experiments carried out for 4 and 49p- and *n*-type polypropylene-based melt mixed composites with single walled carbon nanotubes – which were connected electrically in series and thermally in parallel – TEG models were developed in COMSOL Multiphysics (Fig. 3,4). The models were then validated by comparing simulation results with the measurement results from [27].

For the sample using 4 pairs, and the experiments carried out in the laboratory, 8 strips with dimension of 40 mm × 5 mm × 0.5 mm were cut from melt-processed and compression molded plates which were then mounted on two insulated copper blocks as shown in Fig. 3(A).

Two neighboring strips were connected by graphite foil and the contact was enhanced by using dots of silver paint (white areas). In order to ensure good contact between the cooper blocks and the leg construction, a thermally conductive but electrically insulating paste (GCExtreme Thermal Compound, GELID solutions) was homogenously spread on the inner parts of the copper blocks before the leg construction was mounted on top of it. The two ends of the module were connected by a copper wire to a Keithley DMM 2001 for the measurement of the generated thermovoltage. The copper blocks with the leg construction were inserted in the thermally insulated chamber, the self-made

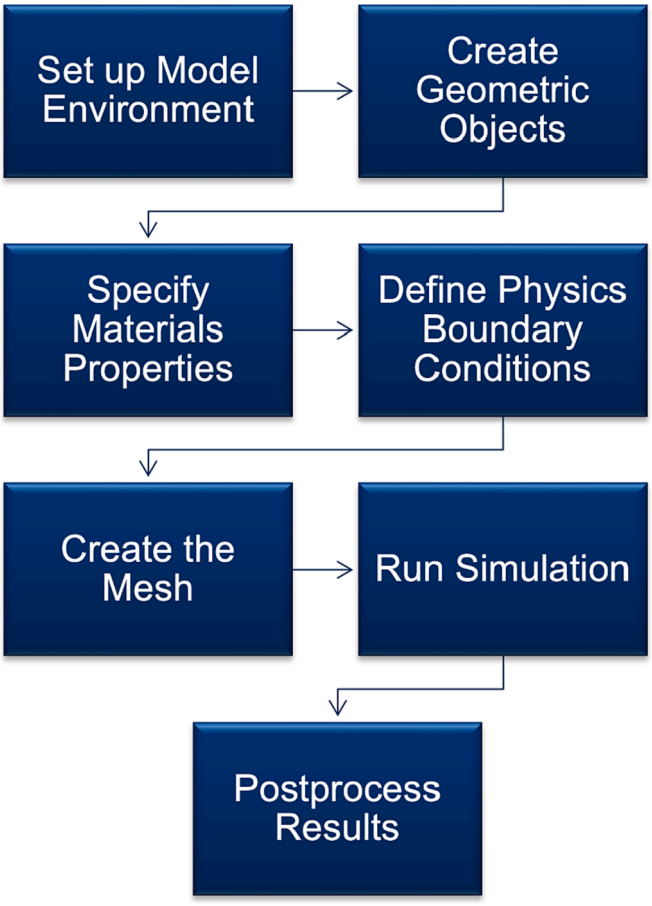

Fig. 2. Simulation flowchart used for the modelling.

Table 1
Electrical properties of PP based composites filled with CNTs and CuO* (data partially taken with permission from reference [27].

Property	Abbreviation	Value		Unit
		n-type	p-type	
Heat capacity at constant pressure	Cp	1.65	1.54	$J/(g^*K)$
Density	ρ	970	930	kg/m^3
Seebeck coefficient	$S(T)$	−56.6+/- 0.46	36.8+/- 1.02	$[\mu V/K]$
Electrical conductivity	$\sigma(T)$	0.24+/- 0.06	0 .17+/- 0.03	$[S/cm]$
Thermal conductivity	$k(T)$	0.48+/- 0.02	0.47 +/- 0.02	$[W/(m.K)]$
Relative permittivity	–	3	3	1

*The exact compositions are: p-type PP-2 wt% SWCNT-5 wt% CuO, *n*-type PP-2 wt% SWCNT-5 wt% CuO-10 wt% PEG.

equipment being designed and constructed in the IPF laboratory [27]. The copper blocks are equipped with a micro-heater and connected to a temperature controller. For the measurements, one copper block was held at the constant temperature of 40 °C, and the temperature of the other copper block was varied up to 110 °C in steps of 10 °C, giving a maximum temperature difference of 70 °C. The internal resistance of this module was 16 kΩ.

For the second example using 49 pairs, strips of the same dimension were cut from the compression molded sheets and an alternating structure was formed. The ends of two neighboring strips were connected by pressing together approximately 1 mm of each strip at 120 °C, a temperature at which the polymer is soft but not completely molten. By this method a good contact between p- and *n*-type strips was ensured and, by repetition, resulted in an accordion-like structure (Fig. 4A). Polyimide films were then inserted between the p- and *n*-type films as insulating layers (Fig. 4B). The ends of the structure were painted with the same GC Extreme (as noted above) to enhance the thermal contact to the copper blocks. The internal resistance of this module was 500 mΩ. The accordion-like structure was then inserted between the two copper blocks and measurements were performed in a similar manner to those described above.

Following on from the dimensions of the strips (40 mm × 5 mm × 0.3 mm) the geometries of the TEG module were defined together with the material properties, the phenomena occurring and the boundary condition of the module. For the simulation two modules in COMSOL were used, '*Heat Transfer in Solids*' and '*Electric Currents*'.

- Heat Transfer in Solids: This interface is often applied to describe heat transfer in solids via conduction, convection, and radiation. A solid model was enabled automatically on all domains, but the software also has the facility to incorporate alternative domain types, such as a fluid domain. In the solid domains, the temperature equation corresponds to the differential form of Fourier's law. This may also include other contributions such as heat sources and when this '*physics*' version of the interface is introduced, the software includes Solid, Thermal Insulation and Initial Values as the default boundary condition. The Initial Values node adds an initial value for the temperature that can serve as an initial condition for a transient simulation or as an initial guess for a nonlinear solver. However, the Thermal Insulation node is the default boundary condition for all Heat Transfer interfaces and this boundary condition means that there is no heat flux transfer across the boundary and hence specifies where the domain is well insulated.
- The Electric Currents: This interface is often applied to compute electric fields, and current and potential distributions in conducting mediums when inductive effects are negligible. The physics of the interface using the scalar electric potential as the dependent variable to solve a current conservation equation based on Ohm's law. The

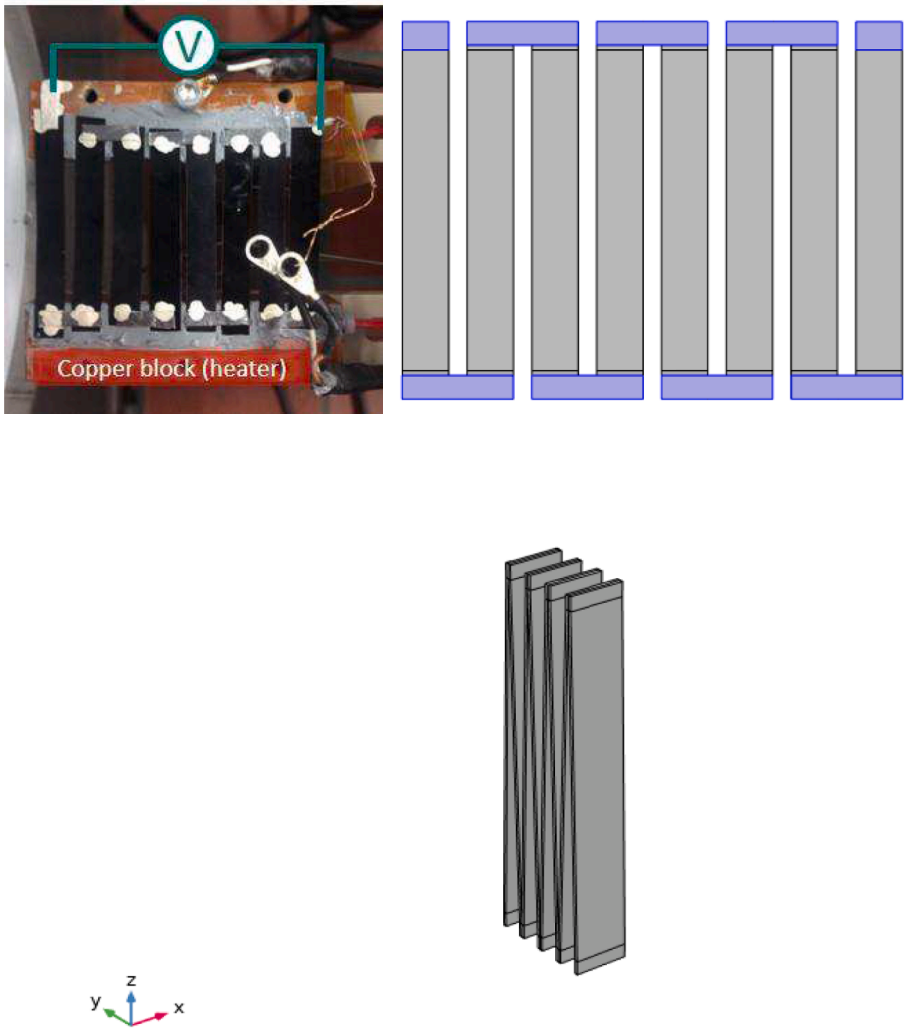

Fig. 3. The demonstration of thermoelectric modules: (A) experiment with 4 thermocouples (adopted with permission from ref. [27], (B) 4 pairs planar model in COMSOL, (C) 4 pairs zigzag model in COMSOL.

main node is Current Conservation, which adds the equation for the electric potential and offers a 'settings' window for defining the electrical conductivity as well as the constitutive relation for the electric displacement field and its associated material properties such as relative permittivity. When using the Electrical Current interface, COMSOL assumes the Current Conservation, Electric Insulation and Initial Values nodes as the default boundary conditions. As a means of simulation control, the Current Conservation node provides an interface for specifying the electric conductivity as well as the constitutive relation and the relative permittivity for the displacement current. The Electric Insulation node, which is the default boundary condition, adds electric insulation and this boundary condition indicates that no electric current flows into the defined boundary.

Mesh study

A number of factors need to be considered when generating the mesh, all of which can be explored using the various features and the software functionality of COMSOL. For example, factors such as selecting a mesh sequence type can either completely automate the process of meshing the geometry or the user can generate create a custom mesh; which then gives control over the order of operations in the meshing sequence, the element types that can be used and the size and distribution of the elements, etc. [56]. It is these aspects that contribute to a user's ability to not only resolve the model geometry correctly but also efficiently because the mesh used in the COMSOL simulation has a significant impact on the modelling requirements and is one of the most memory intensive steps in setting up and solving the finite element problem [57].

Accordingly, for each model, several meshing types were tested and the appropriate mesh was chosen accordingly. For example, Fig. 5 presents the variation of the internal resistance from the 4-pairs TEG Planar model vs the number of elements, and the graph shows that a plateau level of approximately constant internal impedance is reached after a finite number of elements. From which, the number of elements (86002) – a Fine Free Tetrahedral mesh – was selected to ensure a convergence criterion. This is a vital step in the modelling process in order to achieve precise results within the shortest time without a loss in the solution precision. Similarly, for both the 4-pairs zigzag and the 49-pairs modules, a Fine mesh was chosen.

Result and analysis

This research used the COMSOL Multiphysics thermoelectric effect interface and the simulation results (temperature distribution and electric potential differences) for the 4-pair configurations are presented in Fig. 6. The thermoelectric effect, the electromagnetic power

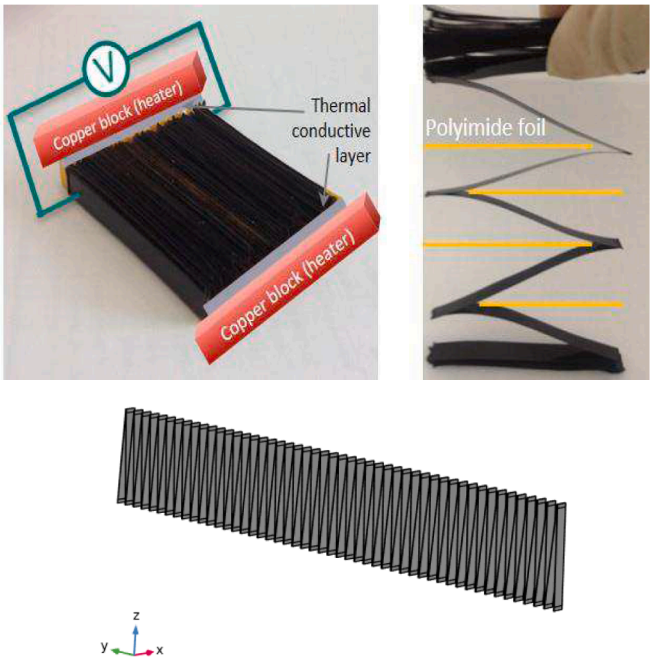

Fig. 4. (A) Experiment with 49 thermocouples (adapted with permission from ref. [27], (B) experiment with 49 thermocouples side view, (C) 49 pairs zigzag model in COMSOL.

dissipation (Joule's effect), and the temperature-dependent electromagnetic material properties are all included in the Multiphysics coupling. Convective heat transmission was not included in this simulation since all surfaces (except the hot and cold connectors) have built-in thermal insulation. Fig. 6–A indicates the temperature distributions of the simulated model in which the thermoelectric elements were thermally connected in parallel and therefore, as shown in Fig. 6–A, the temperature at the top (hot junction, 110 °C) and at the bottom (cold junction, 40 °C) for all the legs is uniform.

The analysis of electric potential is shown in Fig. 6-B. Thermoelectric elements were electrically connected in series and therefore, as can be seen, the voltage potential varies from one side of the models to the other end. For temperature gradient of 70 °C, the electrical potential generated was 26.2 mV. Fig. 6-C and 6-D present the temperature distribution and the distribution of electric potential respectively. The temperature distribution for the zigzag model is the same as the planar model (6-A), however the voltage potential for the zigzag model is slightly lower than the planar model. Similarly, Fig. 7 shows the temperature distribution and the electrical potential of the 49-pair TEG module, respectively.

Fig. 8 presents the thermoelectric output voltage vs the temperature difference for the experimental results for the module with 4 pairs together with the computational results. The cold side temperature was fixed at 40 °C and the temperature of the hot junction steadily increased until it reached 110 °C with electric potential difference measurements being taken for every 10 °C.

The simulation results indicated a slightly higher output voltage than the experimental results and this is because the COMSOL Multiphysics model assumes perfect conditions (i.e., no heat losses from the thermoelectric element to the surrounding environment) as it simulates a thermoelectric generator. In practice, especially at the interfaces between the polymer strips and the copper blocks (planar geometry model) or at the interfaces between p- and *n*-type strips (zigzag geometry model), the electrical contact resistance may be responsible for such deviations because this leads to relatively high internal resistances for the two TEG demonstrators [27].

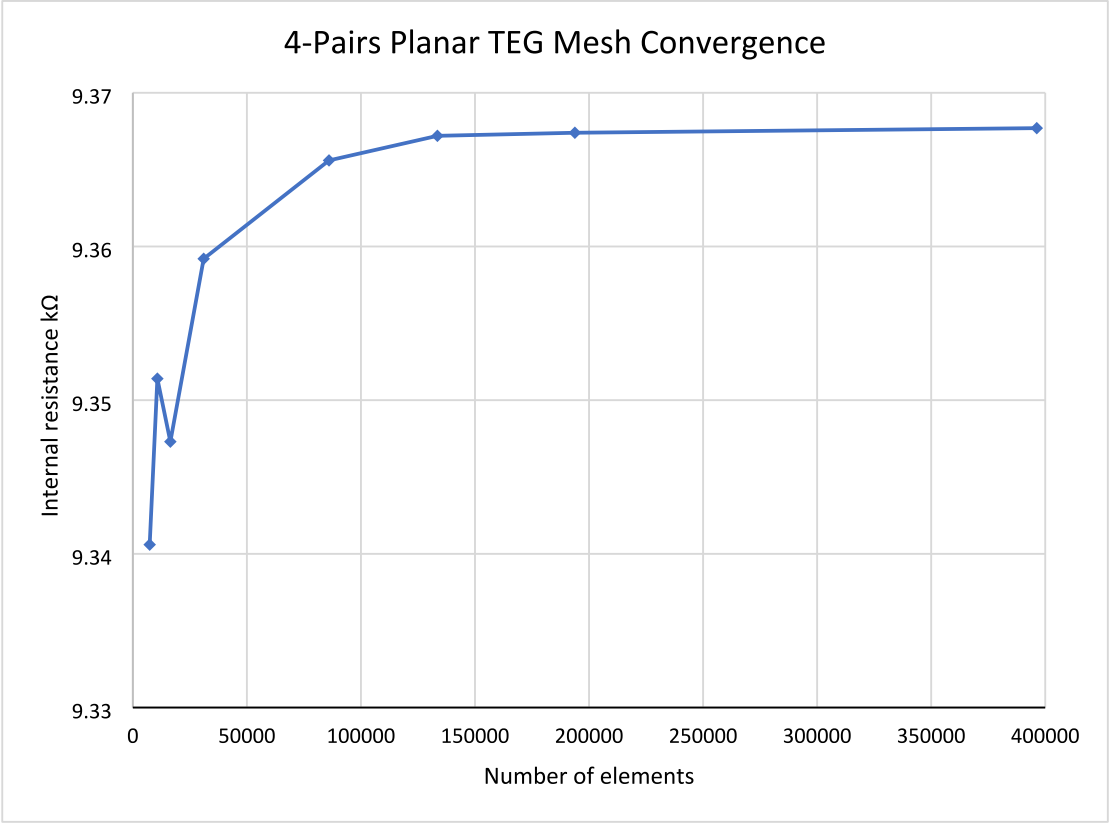

Fig. 5. Variation of TEG internal resistance with different elements numbers.

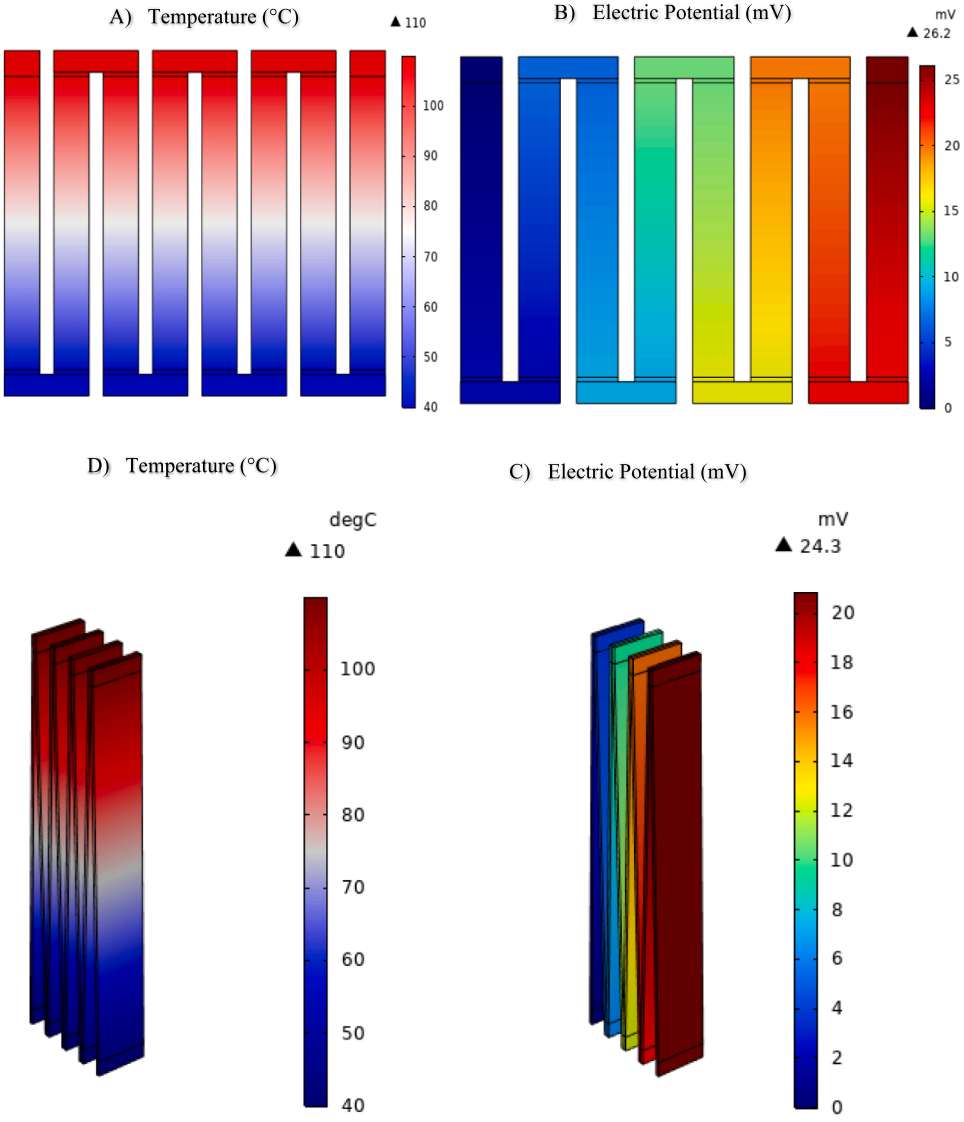

Fig. 6. TEG model for the 4 pair configurations in COMSOL A) temperature distribution for the planar model, B) electric potential difference for the planar model. C) Temperature distribution for the zigzag model, D) electric potential difference for zigzag model.

Even though in the case of the 4-pair demonstrator a silver paste was used to reduce contact resistance, and for the 49-pair demonstrator hot pressing was used to combine the strips, some electrical contact resistance (and so loss) occurred – for which the COMSOL model takes no account. Such contact resistances increase as more pairs and so more interfaces are added, which then also explains why there is a higher difference between the modelled and measured values for 49 pairs than for 4 pairs (Figs. 8, 9). In addition, since the electrical conductivity and the Seebeck coefficient both depend on temperature – and these have been taken as constant values for the simulation – the results indicate that more attention needs to be paid to the problem of contact resistances when producing contact points for a demonstrator.

In general, and especially on the 4-pair demonstrator, it is argued that the computational results (in showing trends with sufficient accuracy), indicate that such models are suitable for these modelled simulation approaches. It will also be noticed that the zigzag model produced less electrical potential in comparison to the planar TEG model, and one suggestion for this is that the planar mode used copper contacts between the p and n legs whilst the zigzag model used no contacts between the p and n legs. Nonetheless, despite these differences, as Fig. 8 indicates, the computational results for the 4-pair configurations are consistent with the experimental results and so underpin the value of this simulation approach to analysis.

Table 2 indicated the Standard and Mean Deviation values. In order to calculate the Standard and Mean deviation, Equations 3 and 4 were used respectively [58,59].

$$\frac{1}{n}\sum_{i=1}^{n}|x_i - m(X)| \tag{3}$$

Where:$m(X)$ = average value of the data set$n$ = number of data valuesx_i = data values in the set

$$\sigma = \sqrt{\frac{\sum (x_i - \mu)^2}{N}}$$

Where:σ = standard deviation$N$ = number of the conducted experimentx_i = each value from the experimentμ = the experiment mean

Conclusions

This study illustrates the research value of using the COMSOL

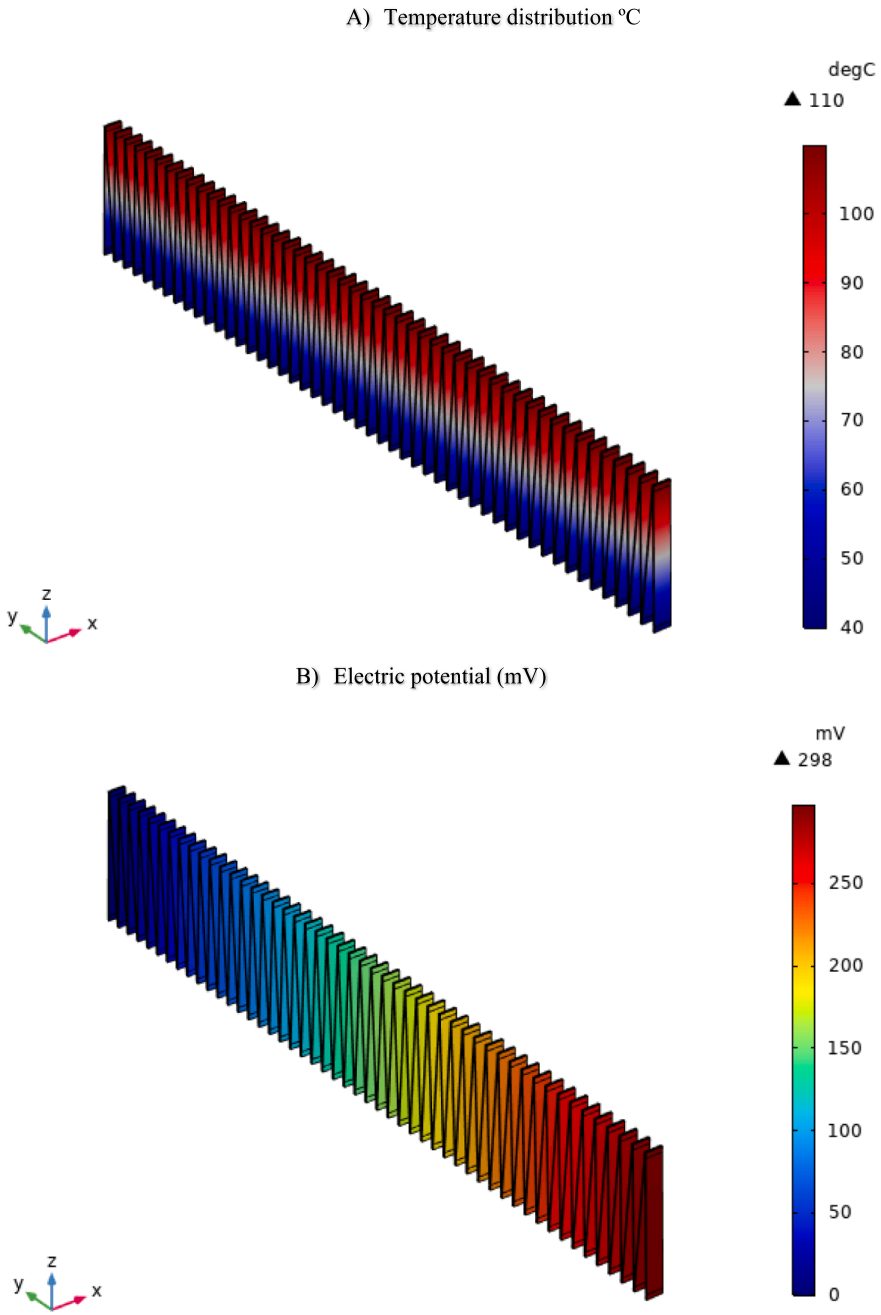

Fig. 7. TEG model for the 49 pair configurations in COMSOL A) temperature distribution B) electric potential difference.

Multiphysics software for simulating the TE behavior of two demonstrators based on *n*-type and p-type polymer composites from the same matrix material (polypropylene) utilising a melt mixing approach. This research is part of the InComEss project, which aims to provide a new environmentally friendly and economically viable method for highly effective energy harvesting. Based on the results of the measurements carried out in the laboratory, TEG models consisting of 4 and 49 pairs of p and *n*-type material strips with different arrangement geometries were developed in COMSOL Multiphysics and validated. In line with the laboratory experiments, the cold side temperature was set at 40 °C, and the hot junction temperature gradually raised until it approached 110 °C. With the 4-pair models it was noted that the electrical potential produced by the planar model was slightly higher than that of the zigzag model. The simulation results of the generated thermovoltages were confirmed by the experimental results. The match being very good for the 4-pair models but not sufficient for the 49-pair assemblies due mainly to the contact resistances at the strip contact points. It should be noted that ideal operating conditions for the TE generator are investigated in the software, taking into account the same dimensions for each of the p and n strips and a uniform electrical conductive layer. Generators developed in the laboratory are manually prepared and combined and may have minor differences. The main objective of the paper was to validate a model that could be used for further analysis of TEG modules (of the same design) but with different material properties – all without the need to produce a prototype. Overall, the results were encouraging and the usefulness of COMSOL Multiphysics software was established for analysis of new small-scale thermoelectric generator geometries in its application to the study of different polymer matrices constructed from conductive polymer composites. Future studies will include combining Thermoelectric and Piezoelectric composite materials into a hybrid Thermo-Piezo Electric Generator (TPEG). This structure will enable each generator to interface with its respective ambient source for

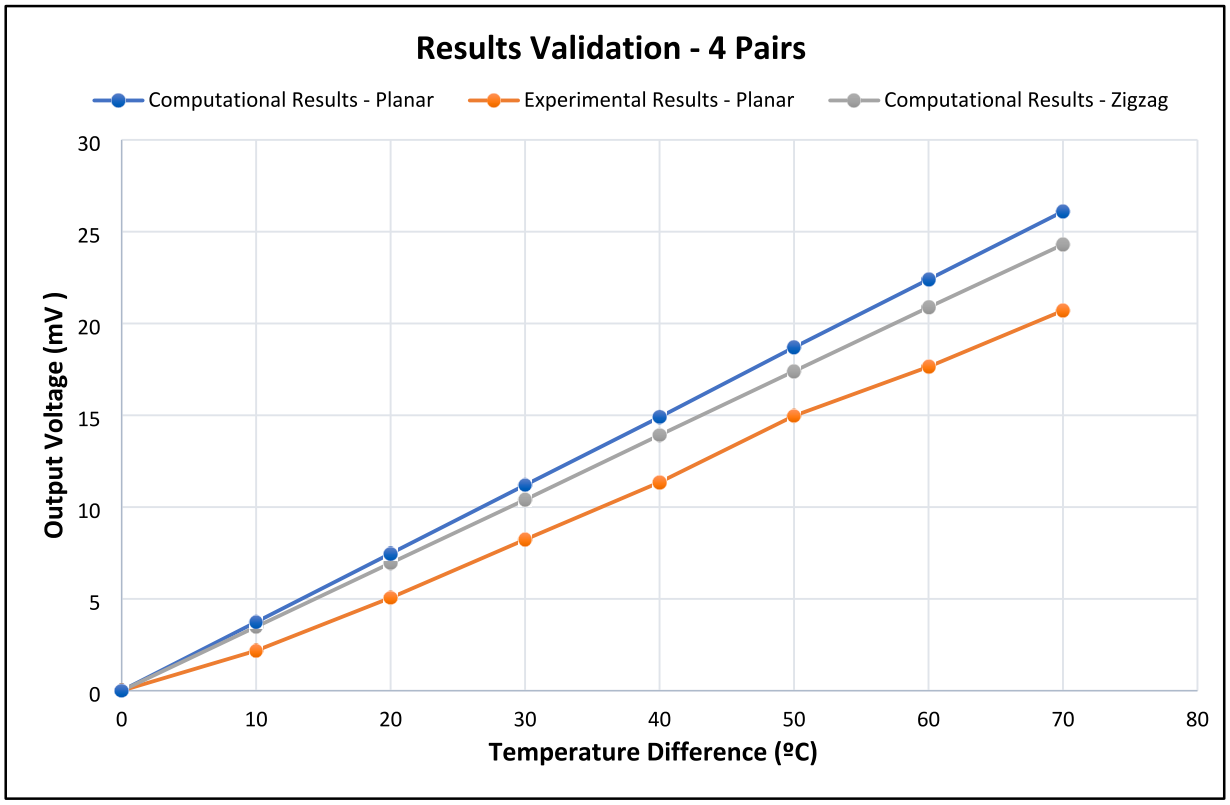

Fig. 8. TEG voltage potential results for experimental values [27] and computational analysis for 4 pairs, for planar and zigzag models.

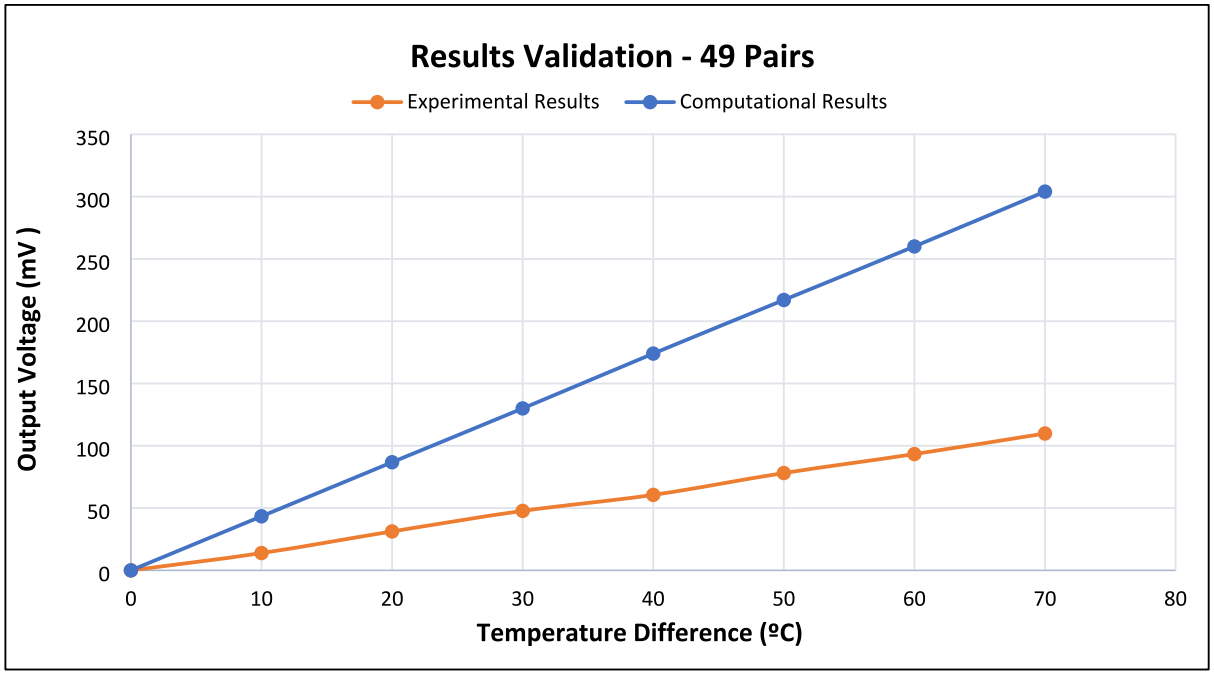

Fig. 9. TEG voltage potential results for experimental values [27] and computational analysis for 49 pairs – zigzag geometry model.

simultaneous power generation and operation simultaneously, overcoming the inconsistency of typical Piezo and Thermoelectric harvesters.

CRediT authorship contribution statement

Qusay Doraghi: Software, Validation, Investigation, Visualization, Writing - original draft. **Alina Żabnieńska-Góra:** Software, Validation, Investigation, Visualization, Conceptualization, Writing - original draft, Writing - review & editing. **Les Norman:** Writing - review & editing.

Table 2
Standard and Mean Deviation values from the experimental data.

Temperature Difference	Standard Deviation		Mean Deviation	
-	49 Pairs	4 Pairs	49 Pairs	4 Pairs
0	0	0	0	0
10	0.506	0.05	0.42	0.03
20	0.295	0.27	0.22	0.20
30	0.322	0.14	0.25	0.10
40	3.589	0.16	2.97	0.11
50	3.910	0.61	3.31	0.46
60	3.893	0.27	3.38	0.21
70	1.716	0.37	1.40	0.26

Beate Krause: Resources, Validation, Investigation, Writing - original draft, Writing - review & editing. **Petra Pötschke:** Resources, Validation, Investigation, Conceptualization, Writing - review & editing. **Hussam Jouhara:** Conceptualization, Investigation, Supervision, Writing - review & editing.

Declaration of Competing Interest

The authors declare that they have no known competing financial interests or personal relationships that could have appeared to influence the work reported in this paper.

Data availability

The data that has been used is confidential.

Acknowledgements

This work has received funding from the European Union's Horizon 2020 Research and Innovation Programme for project InComEss under Grant Agreement Number 862597.

References

[1] B. Egilegor, H. Jouhara, J. Zuazua, F. Al-Mansour, K. Plesnik, L. Montorsi, L. Manzini, ETEKINA: Analysis of the potential for waste heat recovery in three sectors: Aluminium low pressure die casting, steel sector and ceramic tiles manufacturing sector, Int. J. Thermofluids 1-2 (2020), 100002, https://doi.org/10.1016/j.ijft.2019.100002.

[2] M. Venturelli, D. Brough, M. Milani, L. Montorsi, H. Jouhara, Comprehensive numerical model for the analysis of potential heat recovery solutions in a ceramic industry, Int. J. Thermofluids 10 (2021), 100080, https://doi.org/10.1016/j.ijft.2021.100080.

[3] J.J. Fierro, C. Hernández-Gómez, C.A. Marenco-Porto, C. Nieto-Londoño, A. Escudero-Atehortua, M. Giraldo, H. Jouhara, L.C. Wrobel, Exergo-economic comparison of waste heat recovery cycles for a cement industry case study, Energy Convers. Manag. X 13 (2022), 100180, https://doi.org/10.1016/j.ecmx.2022.100180.

[4] T. Korpela, M. Kuosa, H. Sarvelainen, E. Tuliniemi, P. Kiviranta, K. Tallinen, H.-K. Koponen, Waste heat recovery potential in residential apartment buildings in Finland's Kymenlaakso region by using mechanical exhaust air ventilation and heat pumps, Int. J. Thermofluids 13 (2022) 100127.

[5] J.J. Fierro, C. Nieto-Londoño, A. Escudero-Atehortua, M. Giraldo, H. Jouhara, L. C. Wrobel, Techno-economic assessment of a rotary kiln shell radiation waste heat recovery system, Therm. Sci. Eng. Prog. 23 (2021), 100858, https://doi.org/10.1016/j.tsep.2021.100858.

[6] A. Baroutaji, A. Arjunan, M. Ramadan, J. Robinson, A. Alaswad, M. A. Abdelkareem, A.-G. Olabi, Advancements and prospects of thermal management and waste heat recovery of PEMFC, Int. J. Thermofluids 9 (2021), 100064, https://doi.org/10.1016/j.ijft.2021.100064.

[7] A. Zarei, S. Elahi, H. Pahangeh, Design and analysis of a novel solar compression-ejector cooling system with eco-friendly refrigerants using hybrid photovoltaic thermal (PVT) collector, Therm. Sci. Eng. Prog. 32 (October 2021) (2022), https://doi.org/10.1016/j.tsep.2022.101311.

[8] F. Hengel, C. Heschl, F. Inschlag, P. Klanatsky, System efficiency of pvt collector-driven heat pumps, Int. J. Thermofluids 5–6 (2020), 100034, https://doi.org/10.1016/j.ijft.2020.100034.

[9] Y.A.A. Laouid, C. Kezrane, Y. Lasbet, A. Pesyridis, Towards improvement of waste heat recovery systems: a multi-objective optimization of different organic Rankine cycle configurations, Int. J. Thermofluids 11 (2021), 100100, https://doi.org/10.1016/j.ijft.2021.100100.

[10] J. Thaddaeus, G.O. Unachukwu, C.A. Mgbemene, A. Pesyridis, M. Usman, F. A. Alshammari, Design, size estimation, and thermodynamic analysis of a realizable organic Rankine cycle system for waste heat recovery in commercial truck engines, Therm. Sci. Eng. Prog. 22 (January) (2021), 100849, https://doi.org/10.1016/j.tsep.2021.100849.

[11] D. Brough, J. Ramos, B. Delpech, H. Jouhara, Development and validation of a TRNSYS type to simulate heat pipe heat exchangers in transient applications of waste heat recovery, Int. J. Thermofluids 9 (2021), 100056, https://doi.org/10.1016/j.ijft.2020.100056.

[12] M.A. Abdelkareem, H.M. Maghrabie, A.G. Abo-Khalil, O.H.K. Adhari, E.T. Sayed, A. Radwan, H. Rezk, H. Jouhara, A.G. Olabi, Thermal management systems based on heat pipes for batteries in EVs/HEVs, J. Energy Storage 51 (2022) 104384.

[13] V. Guichet, B. Delpech, N. Khordehgah, H. Jouhara, Experimental and theoretical investigation of the influence of heat transfer rate on the thermal performance of a multi-channel flat heat pipe, Energy 250 (2022), 123804, https://doi.org/10.1016/j.energy.2022.123804.

[14] M.A. Abdelkareem, H.M. Maghrabie, E.T. Sayed, E.-C. Kais, A.G. Abo-Khalil, M. A. Radi, A. Baroutaji, A.G. Olabi, Heat pipe-based waste heat recovery systems: background and applications, Therm. Sci. Eng. Prog. 29 (2022), 101221, https://doi.org/10.1016/j.tsep.2022.101221.

[15] B. Abderezzak, S. Randi, Experimental investigation of waste heat recovery potential from car radiator with thermoelectric generator, Therm. Sci. Eng. Prog. 20 (August) (2020), 100686, https://doi.org/10.1016/j.tsep.2020.100686.

[16] H. Jouhara, A. Żabnieńska-Góra, N. Khordehgah, Q. Doraghi, L. Ahmad, L. Norman, B. Axcell, L. Wrobel, S. Dai, Thermoelectric generator (TEG) technologies and applications, Int. J. Thermofluids 9 (2021), 100063, https://doi.org/10.1016/j.ijft.2021.100063.

[17] H. Sahli, M. elakhdar, B. Tashtoush, E. Nahdi, Analysis of a hybrid solar absorption cooling system with thermoelectric generator, Therm. Sci. Eng. Prog. 35 (2022), 101474, https://doi.org/10.1016/j.tsep.2022.101474.

[18] "InComEss." [Online]. Available: https://www.incomess-project.com.

[19] E. Iancu, CRC Thermoelectric Transport Theory, CRC Press, 1995.

[20] P. Qiu, X. Shi, L. Chen, Cu-based thermoelectric materials, Energy Storage Mater. 3 (2016) 85–97, https://doi.org/10.1016/j.ensm.2016.01.009.

[21] N. Jia, J. Cao, X.Y. Tan, J. Dong, H. Liu, C.K.I. Tan, J. Xu, Q. Yan, X.J. Loh, A. Suwardi, Thermoelectric materials and transport physics, Mater. Today Phys. 21 (2021), 100519, https://doi.org/10.1016/j.mtphys.2021.100519.

[22] Z.G. Chen, G. Hana, L. Yanga, L. Cheng, J. Zou, Nanostructured thermoelectric materials: current research and future challenge, Prog. Nat. Sci. Mater. Int. 22 (6) (2012) 535–549, https://doi.org/10.1016/j.pnsc.2012.11.011.

[23] A. Mehdizadeh Dehkordi, M. Zebarjadi, J. He, T.M. Tritt, Thermoelectric power factor: enhancement mechanisms and strategies for higher performance thermoelectric materials, Mater. Sci. Eng. R Reports 97 (2015) 1–22, https://doi.org/10.1016/j.mser.2015.08.001.

[24] J. Mao, Z. Liu, J. Zhou, H. Zhu, Q. Zhang, G. Chen, Z. Ren, Advances in thermoelectrics, Adv. Phys. 67 (2) (2018) 69–147, https://doi.org/10.1080/00018732.2018.1551715.

[25] Bhagyashri Patil, P. Mandon, and E. Prasad, "2021 THERMOELECTRIC GENERATOR (TEG) MARKET. Global Opportunity Analysis and Industry Forecast, 2020-2030," no. October, pp. 1–76, 2021.

[26] N. Jaziri, A. Boughamoura, J. Müller, B. Mezghani, F. Tounsi, M. Ismail, A comprehensive review of thermoelectric generators: technologies and common applications, Energy Rep. 6 (2020) 264–287, https://doi.org/10.1016/j.egyr.2019.12.011.

[27] J. Luo, G. Cerretti, B. Krause, L. Zhang, T. Otto, W. Jenschke, M. Ullrich, W. Tremel, B. Voit, P. Pötschke, Polypropylene-based melt mixed composites with singlewalled carbon nanotubes for thermoelectric applications: Switching from p-type to n-type by the addition of polyethylene glycol, Polymer (Guildf) 108 (2017) 513–520, https://doi.org/10.1016/J.POLYMER.2016.12.019.

[28] R. Kroon, D.A. Mengistie, D. Kiefer, J. Hynynen, J.D. Ryan, L. Yu, C. Müller, Thermoelectric plastics: from design to synthesis, processing and structure–property relationships, Chem. Soc. Rev. 45 (22) (2016) 6147–6164, https://doi.org/10.1039/C6CS00149A.

[29] S. Han, S. Chen, F. Jiao, Insulating polymers for flexible thermoelectric composites: a multi-perspective review, Compos. Commun. 28 (Dec. 2021), 100914, https://doi.org/10.1016/J.COCO.2021.100914.

[30] S. Peng, et al., A review on organic polymer-based thermoelectric materials, J. Polym. Environ. 25 (4) (Dec. 2017) 1208–1218, https://doi.org/10.1007/S10924-016-0895-Z/FIGURES/7.

[31] M. Culebras, C. Gómez, A. Cantarero, Review on polymers for thermoelectric applications, Materials 7 (9) (2014) 6701–6732, https://doi.org/10.3390/ma7096701.

[32] M.A. Kamarudin, S.R. Sahamir, R.S. Datta, B.D. Long, M.F. Mohd Sabri, S. Mohd Said, A review on the fabrication of polymer-based thermoelectric materials and fabrication methods, Sci. World J. 2013 (2013) 1–17, https://doi.org/10.1155/2013/713640.

[33] C.A. Hewitt, A.B. Kaiser, S. Roth, M. Craps, R. Czerw, D.L. Carroll, Multilayered carbon nanotube/polymer composite based thermoelectric fabrics, Nano Lett. 12 (3) (Mar. 2012) 1307–1310, https://doi.org/10.1021/NL203806Q/SUPPL_FILE/NL203806Q_SI_001.PDF.

[34] C.A. Hewitt, D.S. Montgomery, R.L. Barbalace, R.D. Carlson, D.L. Carroll, Improved thermoelectric power output from multilayered polyethylenimine doped carbon nanotube based organic composites, J. Appl. Phys. 115 (18) (May 2014), 184502, https://doi.org/10.1063/1.4874375.

[35] W. Bauhofer, J.Z. Kovacs, A review and analysis of electrical percolation in carbon nanotube polymer composites, Compos. Sci. Technol. 69 (10) (2009) 1486–1498, https://doi.org/10.1016/J.COMPSCITECH.2008.06.018.
[36] B. Krause, C. Barbier, J. Levente, M. Klaus, P. Pötschke, Screening of different carbon nanotubes in melt-mixed polymer composites with different polymer matrices for their thermoelectrical properties, *J. Compos. Sci.* 3 (4) (2019) 106, https://doi.org/10.3390/JCS3040106.
[37] Z. Antar, J.F. Feller, H. Noël, P. Glouannec, K. Elleuch, Thermoelectric behaviour of melt processed carbon nanotube/graphite/poly(lactic acid) conductive biopolymer nanocomposites (CPC), Mater. Lett. 67 (1) (2012) 210–214, https://doi.org/10.1016/J.MATLET.2011.09.060.
[38] L. Tzounis, T. Gärtner, M. Liebscher, P. Pötschke, M. Stamm, B. Voit, G. Heinrich, Influence of a cyclic butylene terephthalate oligomer on the processability and thermoelectric properties of polycarbonate/MWCNT nanocomposites, Polymer (Guildf) 55 (21) (2014) 5381–5388, https://doi.org/10.1016/J.POLYMER.2014.08.048.
[39] Y.C. Sun, D. Terakita, A.C. Tseng, H.E. Naguib, Study on the thermoelectric properties of PVDF/MWCNT and PVDF/GNP composite foam, Smart Mater. Struct. 24 (8) (2015), 085034, https://doi.org/10.1088/0964-1726/24/8/085034.
[40] J. Luo, B. Krause, P. Pötschke, J. Luo, B. Krause, P. Pötschke, Melt-mixed thermoplastic composites containing carbon nanotubes for thermoelectric applications, *AIMS Mater. Sci.* 3 (3) (2016) 1107–1116, https://doi.org/10.3934/MATERSCI.2016.3.1107.
[41] B. Krause, V. Bezugly, V. Khavrus, L. Ye, G. Cuniberti, P. Pötschke, Boron doping of SWCNTs as a way to enhance the thermoelectric properties of melt-mixed polypropylene/SWCNT composites, *Energies* 13 (2) (2020) 394, https://doi.org/10.3390/EN13020394.
[42] J. Luo, B. Krause, P. Pötschke, "Polymer-Carbon nanotube composites for thermoelectric applications ARTICLES YOU MAY BE INTERESTED IN Polymer-Carbon Nanotube Composites for Thermoelectric Applications," in *32nd International Conference of the POLYMER PROCESSING SOCIETY (PPS32)*, 1914, p. 30001, doi: 10.1063/1.5016688.
[43] P. Pötschke, B. Krause, J. Luo, Melt mixed composites of polypropylene with singlewalled carbon nanotubes for thermoelectric applications: switching from p- to n-type behavior by additive addition, AIP Conf. Proc. 2055 (1) (2019), 090004, https://doi.org/10.1063/1.5084882.
[44] B. Krause, I. Konidakis, M. Arjmand, U. Sundararaj, R. Fuge, M. Liebscher, S. Hampel, M. Klaus, E. Serpetzoglou, E. Stratakis, P. Pötschke, Nitrogen-doped carbon nanotube/polypropylene composites with negative Seebeck coefficient, *J. Compos. Sci.* 4 (1) (2020) 14, https://doi.org/10.3390/JCS4010014.
[45] A.J. Paleo, B. Krause, M.F. Cerqueira, M. Melle-Franco, P. Pötschke, A.M. Rocha, Thermoelectric properties of polypropylene carbon nanofiber melt-mixed composites: exploring the role of polymer on their Seebeck coefficient, Polym. J. 53 (10) (2021) 1145–1152, https://doi.org/10.1038/s41428-021-00518-7.
[46] A.J. Paleo, B. Krause, M.F. Cerqueira, E. Muñoz, P. Pötschke, A.M. Rocha, Nonlinear thermopower behaviour of N-type carbon nanofibres and their melt mixed polypropylene composites, Polymers (Basel) 14 (2) (2022), https://doi.org/10.3390/POLYM14020269.
[47] O. Voigt, B. Krause, P. Pötschke, M.T. Müller, S. Wießner, Thermoelectric performance of polypropylene/carbon nanotube/ionic liquid composites and its dependence on electron beam irradiation, *J. Compos. Sci.* 6 (1) (2022) 25, https://doi.org/10.3390/JCS6010025.
[48] M. Piao, M.R. Alam, G. Kim, U. Dettlaff-Weglikowska, S. Roth, Effect of chemical treatment on the thermoelectric properties of single walled carbon nanotube networks, Phys. Status Solidi Basic Res. 249 (12) (2012) 2353–2356, https://doi.org/10.1002/PSSB.201200101.
[49] "The COMSOL Product Suite," https://www.comsol.com/products.
[50] S. Addanki, D. Nedumaran, Simulation and fabrication of thermoelectric generators for hand held electronic gadgets, Mater. Sci. Eng. B 251 (Dec. 2019), 114453, https://doi.org/10.1016/J.MSEB.2019.114453.
[51] D. Luo, R. Wang, Y. Yan, Z. Sun, W. Zhou, R. Ding, Comparison of different fluid-thermal-electric multiphysics modeling approaches for thermoelectric generator systems, Renew. Energy 180 (Dec. 2021) 1266–1277, https://doi.org/10.1016/J.RENENE.2021.09.033.
[52] D. Luo, R. Wang, Y. Yan, W. Yu, W. Zhou, Transient numerical modelling of a thermoelectric generator system used for automotive exhaust waste heat recovery, Appl. Energy 297 (Sep. 2021), 117151, https://doi.org/10.1016/J.APENERGY.2021.117151.
[53] K. Charilaou, T. Kyratsi, L.S. Louca, Design of an air-cooled thermoelectric generator system through modelling and simulations, for use in cement industries, Mater. Today Proc. 44 (2021) 3516–3524, https://doi.org/10.1016/J.MATPR.2020.11.392.
[54] T. Ma, X. Lu, J. Pandit, S.V. Ekkad, S.T. Huxtable, S. Deshpande, Q.-W. Wang, Numerical study on thermoelectric–hydraulic performance of a thermoelectric power generator with a plate-fin heat exchanger with longitudinal vortex generators, Appl. Energy 185 (2017) 1343–1354.
[55] X. Wang, J.i. Qi, W. Deng, G. Li, X. Gao, L. He, S. Zhang, An optimized design approach concerning thermoelectric generators with frustum-shaped legs based on three-dimensional multiphysics model, Energy 233 (2021), 120810, https://doi.org/10.1016/J.ENERGY.2021.120810.
[56] Q. Doraghi, et al., Investigation and Computational Modelling of Variable TEG Leg Geometries, ChemEngineering 5 (3) (2021), https://doi.org/10.3390/chemengineering5030045.
[57] Comsol, "COMSOL Multiphysics Application Library.".
[58] T. Pham-Gia, T.L. Hung, The mean and median absolute deviations, Math. Comput. Model. 34 (7–8) (2001) 921–936, https://doi.org/10.1016/S0895-7177(01)00109-1.
[59] Sheldon M. Ross, *Introductory Statistics*, 3rd ed. 2010.